Determination of Anand constants for SAC Solders using Stress-Strain or Creep Data

Mohammad Motalab, Zijie Cai, Jeffrey C. Suhling, Pradeep Lall
Center for Advanced Vehicle Electronics
Auburn University
Auburn, AL 36849
Phone: +1-334-844-3332
FAX: +1-334-844-3307
E-Mail: jsuhling@eng.auburn.edu

ABSTRACT
The Anand viscoplastic constitutive model is often used to represent the deformation behavior of solders in electronic assemblies. In the Anand model, plasticity and creep are unified and described by the same set of flow and evolution relations. The nine parameters of the Anand constitutive model are typically determined from uniaxial stress-strain tests at several strain rates and temperatures using a standard multistep model parameter determination procedure. Conversely, creep data are often measured for solders, but typically are not used to determine Anand model constants.

In this study, the theoretical equations for the uniaxial stress-strain response (constant strain rate) and for the creep response of solder have been derived from the Anand viscoplastic model. Procedures for extracting the Anand model constants from experimental stress-strain and creep data were also established. The two developed methods were then applied to find the Anand constants for SAC305 (Sn-3.0Ag-0.5Cu) lead free solder using two completely different sets of experimental test data. The first set of Anand parameters were extracted from uniaxial stress strain data measured over a wide range of strain rates ($\dot{\varepsilon}$ = 0.001, 0.0001, and 0.00001 1/sec) and temperatures (T = 25, 50, 75, 100, and 125 ^{o}C). The second set of Anand parameters were calculated from creep test data measured at several stress levels (σ = 10, 12 and 15 MPa and temperatures (T = 25, 50, 75, 100, and 125 ^{o}C).

The two sets of Anand model constants derived from the stress-strain and creep data have been compared and found to be numerically very similar in magnitude. In addition, the accuracy (goodness of fit) of the Anand model using the extracted material constants has been evaluated by comparing the responses calculated from the Anand model with the measured stress-strain and creep data. In all cases, the Anand model was shown to represent the observed data very well over a wide range of temperatures and stress/strain levels.

INTRODUCTION
Solder joint fatigue is one of the predominant failure mechanisms in electronic assemblies exposed to thermal cycling. Reliable, consistent, and comprehensive solder constitutive equations and material properties are needed for use in mechanical design, reliability assessment, and process optimization. The primary goal of thermo-mechanical analyses in the electronic industry is to be able to predict the reliability of the solder joints before extensive testing. Although many constitutive models have been used for Sn-Pb and lead free solders, the Anand model has been very popular because of its ability to model both plasticity and creep, and because it has been embedded in several commercial finite element codes.

A review of lead free solders mechanical behavior and mechanical properties has been presented by Ma, et al. [1]. They showed that it is very important to use aging dependent viscoplastic constitutive equations for Sn-Ag-Cu (SAC) lead free solders. The literature contains a wide variety of approaches for constitutive modeling of microelectronic solders. For example, a simple power law was employed by Solomon [2] to characterize the relationship of shear stress, shear strain and shear strain rate. He showed that a high Pb content solder was less temperature dependent and less strain rate sensitive than Sn-Pb solder. Based on continuum theory, Busso, et al. [3] presented a visco-plastic model that accounted for the stress-dependence of the activation energy and the strong Bauschinger effect for Sn-Pb solder. The kinematic hardening rule in plastic flow was considered in their model, but isotropic hardening and static recover terms were ignored.

Sung and coworkers [4] developed a new viscoplastic model for Sn-Pb solder by combining grain boundary sliding and matrix dislocation deformation mechanisms, emphasizing the effects of grain and phase sizes on thermal fatigue life of eutectic solder joints. They also introduced different evolution equations of the internal stress tensor to describe the transient behaviors during tensile testing and first stage creep. Qian, et al. [5] employed the back stress to describe the transient stage of a stress-strain curve in a unified constitutive model for Sn-Pb solder. Skipor [6] employed the Bodner-Partom constitutive relations to represent the internal inelastic deformation for the solder with eutectic composition.

Chen, et al. [7] presented a constitutive model with a kinematic hardening rule for Sn-Pb solder and employed it to simulate the isothermal cyclic behavior under uniaxial and torsional loading. An implicit constitutive integration scheme was presented for inelastic flow of solder. Darveaux and Banerji [8] developed a hyperbolic sine type power-law constitutive model for Sn based solders, which could describe creep flow for both low and high stresses. Pang, et al. [9] performed experiments that showed that Young's modulus

and yield stress of Sn-Pb solder are highly dependent on temperature and strain rate.

Eutectic or near eutectic tin-lead (Sn-Pb) solder (melting temperature TM = 183 °C) has been the predominant choice of the electronics industry for decades due to its outstanding solderability and reliability. So there is a great deal of experimental and theoretical effort to describe the constitutive relationships for Sn-Pb solders. However, legislation that mandates the banning of lead in electronics has been actively pursued worldwide during the last 15 years due to the environmental and health concerns. Although the implementation deadlines and products covered by such legislation continue to evolve, it is clear that laws requiring conversion to lead-free electronics are becoming a reality. Other factors that are affecting the push towards the elimination of lead in electronics are the market differentiation and advantage being realized by companies producing so-called “green” products that are lead-free.

Anand, et al. [10-11] proposed a popular set of viscoplastic constitutive equations for rate-dependent deformation of metals at high temperatures (e.g. in excess of a homologous temperature of $0.5T_m$). Although it was originally aimed at hotworking of high strength aluminum and other structural metals, the so-called Anand model has been adopted successfully to represent isotropic materials such as microelectronic solders (SnPb and lead free) with small elastic deformations and large viscoplastic deformations.

A large number of researchers have used the Anand model for electronic packaging applications. For example, Che, et al. [12] have demonstrated four different constitutive models for the Sn-3.8Ag-0.7Cu solder alloy including elastic-plastic, elastic-creep, elastic plastic with creep, and the viscoplastic Anand model. They showed that the Anand model was consistent with fatigue life predictions for lead free solders. Pei, et al. [13] performed monotonic tensile tests at a wide range of different temperatures and strain rates with two types of lead free solders (Sn3.5Ag and Sn3.8Ag0.7Cu) to get the material parameters of the Anand constitutive model. They showed that using temperature dependent values of the nine constants in the model gave better matching with the experimental results. Mysore and coworkers [14] conducted double lap shear tests on Sn3.0Ag0.5Cu solder alloy and used the results to fit the materials constants in the Anand model. They reported there were significant differences in results obtained with bulk samples and those found with solder joint specimens. A modified Anand Constitutive model was proposed by Chen, et al. [15] that involved using temperature dependent values of one of the model parameters (h_o). Amagai, et al. [16] have established values for the Anand model constants for Sn3.5Ag0.75Cu and SAC105 (Snl.0Ag0.5Cu) lead free solders. In their work, one of the nine required constants was ignored (s_o), and only 8 were specified. Kim, et al. [17] presented values for all 9 constants for SAC105 lead free solder. A modified Anand model was presented by Bai, et al. [18] for SAC305 (Sn3.0Ag0.5Cu) and Sn3.5Ag0.7Cu lead free solders. Their approach employed temperature and strain rate dependent values of for one of the model parameters (h_o). The Anand model has also been widely used in the finite element simulation of solder interconnection in electronic components [19-22].

Review of the various papers in the literature shows that there is little consistency in the values of the Anand model constants derived by different researchers for various SAC solders. It is also evident that large discrepancies in the calculated model constants exist between various research groups for the same SAC alloy. The nine parameters of the Anand constitutive model are typically determined from uniaxial stress-strain tests at several strain rates and temperatures using a standard multistep model parameter determination procedure. Conversely, creep data are often measured for solders, but typically are not used to determine Anand model constants.

In this study, the theoretical equations for the uniaxial stress-strain response (constant strain rate) and for the creep response of solder have been derived from the Anand viscoplastic model. Procedures for extracting the Anand model constants from experimental stress-strain and creep data were also established. The two developed methods were then applied to find the Anand constants for SAC305 (Sn-3.0Ag-0.5Cu) lead free solder using two completely different sets of experimental test data. The first set of Anand parameters were extracted from uniaxial stress strain data measured over a wide range of strain rates ($\dot{\varepsilon}$ = 0.001, 0.0001, and 0.00001 1/sec) and temperatures (T = 25, 50, 75, 100, and 125 ^{o}C). The second set of Anand parameters were calculated from creep test data measured at several stress levels (σ = 10, 12 and 15 MPa and temperatures (T = 25, 50, 75, 100, and 125 ^{o}C). The two sets of Anand model constants derived from the stress-strain and creep data have been compared, and the accuracy (goodness of fit) of the Anand model using the extracted material constants has been evaluated by comparing the responses calculated from the Anand model with the measured stress-strain and creep data.

EXPERIMENTAL PROCEDURE

Uniaxial Test Sample Preparation

Solder uniaxial samples are often fabricated by machining of bulk solder material, or by melting of solder paste in a mold. Use of a bulk solder bars is undesirable, because they will have significantly different microstructures than those present in the small solder joints used in microelectronics assembly. In addition, machining can develop residual stresses in the specimen, and heat generated during turning operations can cause localized microstructural changes on the exterior of the specimens. Reflow of solder paste in a mold causes challenges with flux removal, minimization of voids, microstructure control, and extraction of the sample from the mold. In addition, many of the developed specimens have shapes that significantly deviate from being long slender rods. Thus, undesired non-uniaxial stress states will be produced during loading. Other investigators have attempted to extract constitutive properties of solders by direct shear or tensile

loading or indenting of actual solder joints (e.g. flip chip solder bumps or BGA solder balls). While such approaches are attractive because the true solder microstructure is involved, the unavoidable non-uniform stress and strain states in the joint make the extraction of the correct mechanical properties and stress-strain curves from the recorded load-displacement data very challenging. Also it can be difficult to separate the various contributions to the observed behavior from the solder material and other materials in the assembly (bond pads, silicon die, PCB/substrate, etc.).

In the current study, we have avoided many of the specimen preparation pitfalls identified above by a using a novel procedure where solder uniaxial test specimens are formed in high precision rectangular cross-section glass tubes using a vacuum suction process. The tubes are first cooled by water quenching. They are then sent through a SMT reflow at a later time to re-melt the solder in the tubes and subject them to any desired temperature profile (i.e. same as actual solder joints).

The solder is first melted in a quartz crucible using a pair of circular heating elements (see Figure 1). A thermocouple attached on the crucible and a temperature control module is used to direct the melting process. One end of the glass tube is inserted into the molten solder, and suction is applied to the other end via a rubber tube connected to the house vacuum system. The suction forces are controlled through a regulator on the vacuum line so that only a desired amount of solder is drawn into the tube. The specimens are then cooled to room temperature using a user-selected cooling profile.

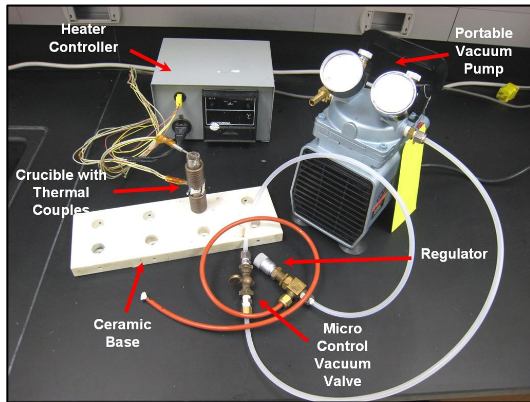

Figure 1 - Specimen Preparation Hardware

In order to see the extreme variations possible in the mechanical behavior and microstructure, we are exploring a large spectrum of cooling rates including water quenching of the tubes (fast cooling rate), air cooling with natural and forced convection (slow cooling rates), and controlled cooling using a surface mount technology solder reflow oven. Typical temperature versus time plots for water quenching and air cooling of the test samples are shown in Figure 2. For the reflow oven controlled cooling, the tubes are first cooled by water quenching, and they are then sent through a reflow oven (9 zone) to re-melt the solder in the tube and subject it to the desired temperature profile. Thermocouples are attached to the glass tubes and monitored continuously using a radio-frequency temperature profiling system to ensure that the samples are formed using the desired temperature profile (same as actual solder joints). Figure 3 illustrates the reflow temperature profile used in this work for Sn-Ag-Cu (SAC) solder specimens.

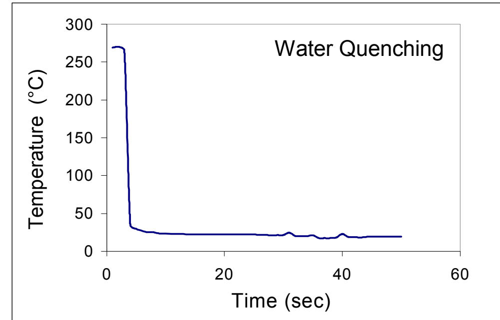

(a) Water Quenched

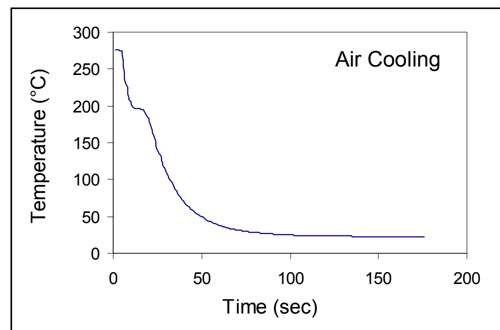

(b) Air Cooled

Figure 2 - Sample Cooling Profiles

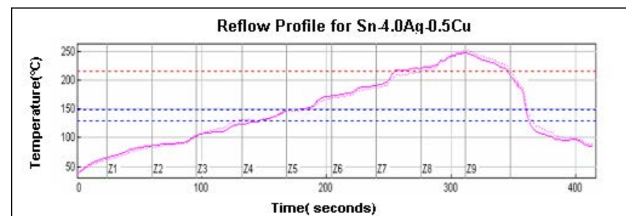

Figure 3 - SAC Reflow Temperature Profile

Typical glass tube assemblies filled with solder and a final extracted specimen are shown in Figure 4. For some cooling rates and solder alloys, the final solidified solder samples can be easily pulled from the tubes due to the differential expansions that occur when cooling the low CTE glass tube and higher CTE solder alloy. Other options for more destructive sample removal involve breaking the glass or chemical etching of the glass. The final test specimen dimensions are governed by the useable length of the tube that can be filled with solder, and the cross-sectional dimensions of the hole running the length of the tube. In the current work, we formed uniaxial samples with nominal dimensions of 80 x 3 x 0.5 mm. A thickness of 0.5 mm was chosen because it matches the height of typical BGA solder balls.

The specimens were stored in the aging oven immediately after the reflow process to eliminate possible room temperature aging effects.

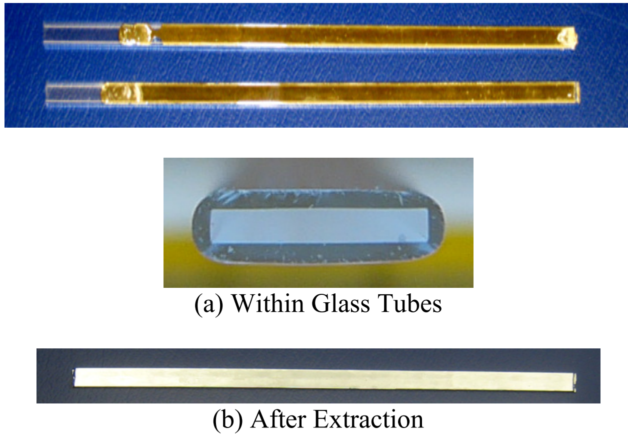

(a) Within Glass Tubes

(b) After Extraction

Figure 4 - Solder Uniaxial Test Specimens

The described sample preparation procedure yielded repeatable samples with controlled cooling profile (i.e. microstructure), oxide free surface, and uniform dimensions. By extensively cross-sectioning several specimens, we have verified that the microstructure of any given sample is very consistent throughout the volume of the sample. In addition, we have established that our method of specimen preparation yields repeatable sample microstructures for a given solidification temperature profile. Samples were inspected using a micro-focus x-ray system to detect flaws (e.g. notches and external indentations) and/or internal voids (non-visible). Figure 5 illustrates results for good and poor specimens. With proper experimental techniques, samples with no flaws and voids were generated.

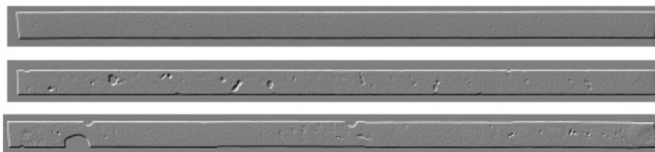

Figure 5 - X-Ray Inspection of Solder Test Specimens (Good and Bad Samples)

Mechanical Testing System

The tension/torsion thermo-mechanical test system as shown in Figure 6 has been used to test the samples in this study. The system provides an axial displacement resolution of 0.1 micron and a rotation resolution of 0.001°. Testing can be performed in tension, shear, torsion, bending, and in combinations of these loadings, on small specimens such as thin films, solder joints, gold wire, fibers, etc. Cyclic (fatigue) testing can also be performed at frequencies up to 5 Hz. In addition, a universal 6-axis load cell was utilized to simultaneously monitor three forces and three moments/torques during sample mounting and testing. Environmental chambers added to the system allow samples to be tested over a temperature range of -185 to +300 °C.

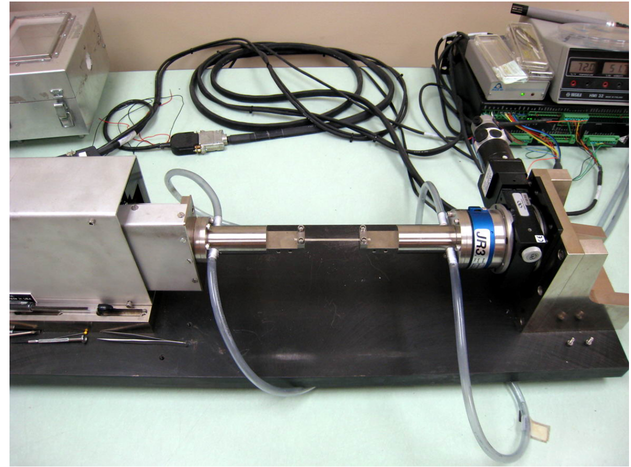

Figure 6 - Mechanical Testing System with Solder Sample

During uniaxial testing, forces and displacements were measured. The axial stress and axial strain were calculated from the applied force and measured cross-head displacement using

$$\sigma = \frac{F}{A} \qquad \varepsilon = \frac{\Delta L}{L} = \frac{\delta}{L} \tag{1}$$

where σ is the uniaxial stress, ε is the uniaxial strain, F is the measured uniaxial force, A is the original cross-sectional area, δ is the measured crosshead displacement, and L is the specimen gage length (initial length between the grips). Finite element analysis of the load train design has shown that the instrument compliance is very small relative to that of the specimen, so that the strain is the sample can be calculated accurately using only the cross-head displacement (less than 0.1% error). The gage length of the specimens in this study was 60 mm, so that the specimen length to width aspect ratio was 20 to 1 (insuring true uniaxial stress states).

Typical Test Data

A typical recorded tensile stress strain curve for solder with labeled standard material properties is shown in Figure 7. The notation "E" is taken to be the effective elastic modulus, which is the initial slope of the stress-strain curve. Since solder is viscoplastic, this effective modulus will be rate dependent, and will approach the true elastic modulus as the testing strain rate approaches infinity. The yield stress σ_Y (YS) is taken to be the standard .2% yield stress (upon unloading, the permanent strain is equal to $\varepsilon = .002$). Finally, the ultimate tensile strength σ_u (UTS) is taken to be the maximum stress realized in the stress-strain data. As shown in Figure 7, the solders tested in this work illustrated nearly perfect elastic-plastic behavior (with the exception of a small transition region connecting the elastic and plastic regions). As the strain level becomes extremely high and failure is imminent, extensive localized necking takes place. These visible reductions in cross-sectional area lead to non-uniform

stress-states in the specimen and drops in the applied loading near the end of the stress-strain curve.

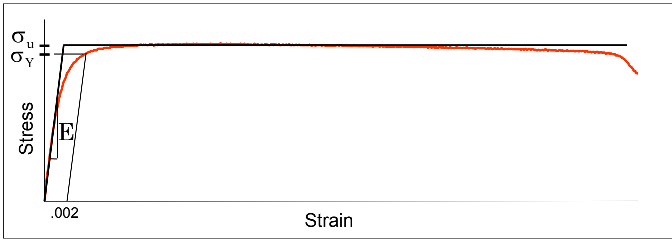

Figure 7 - Typical Solder Stress-Strain Curve

Figure 8 illustrates a typical solder creep curve (strain vs. time response for a constant applied stress). The response begins with a quick transition to the initial "elastic" strain level, followed by regions of primary, secondary, and tertiary creep. Depending on the applied stress level, the primary creep region can be more extensive for the SAC alloys relative to Sn-Pb solders. The secondary creep region is typically characterized by a very long duration of nearly constant slope. This slope is referred to as the "steady state" secondary creep rate or creep compliance, and it is often used by practicing engineers as one of the key material parameters for solder in finite element simulations used to predict solder joint reliability. In this work, the measured creep rates were taken to be the minimum slope values in the secondary creep regions of the observed $\dot{\varepsilon}$ versus t responses. The tertiary creep region occurs when rupture is imminent, and typically features an abrupt change to a nearly constant but significantly increased creep rate.

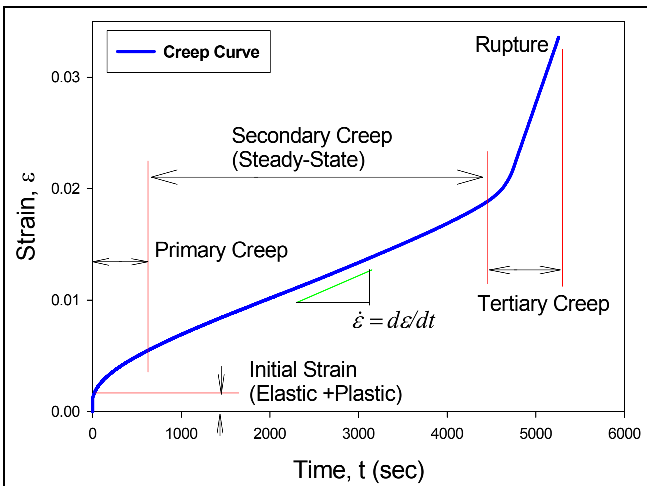

Figure 8 - Typical Solder Creep Curve

Stress-Strain Data Processing

For the uniaxial stress-strain tests, a total of 10 specimens have been tested at each set of test conditions. From the recorded stress-strain data, a set of averaged material properties were extracted. Variations of the average mechanical properties (elastic modulus, yield stress, ultimate strength, creep compliance, etc.) with temperature were observed and then modeled as a function of temperature. In our prior work, we have demonstrated that it is possible to replace a set of 10 recorded stress-strain curves for a certain testing configuration with a single "average" curve that accurately represents the observed response for all strain levels. Although, several different empirical models can be used to represent the observed stress-strain data for solder, we have chosen to use a four parameter hyperbolic tangent model

$$\sigma = C_1 \tanh(C_2\varepsilon) + C_3 \tanh(C_4\varepsilon) \qquad (2)$$

where C_1, C_2, C_3, C_4 are material constants to be determined through regression fitting of the model to experimental data. The initial (zero strain) effective elastic modulus E and UTS can be calculated from the model constants using:

$$E = \sigma'(0) = C_1C_2 + C_3C_4$$
$$UTS = \sigma(\infty) = C_1 + C_3 \qquad (3)$$

Figure 9 illustrates a set of example stress-strain curves for a SAC lead free solder tested under similar environmental and aging conditions, and the corresponding fit of eq. 2 to the data. The excellent representation provided by the elastic-plastic empirical model suggests that it indeed provides a mathematical description of a suitable "average" stress-strain curve for a set of experimental curves measured under fixed test conditions. We have extensive stress-strain data for SAC lead free and Sn-Pb Solders [23-28], and have demonstrated the model in eq. (2) works extremely well for all alloys and temperatures.

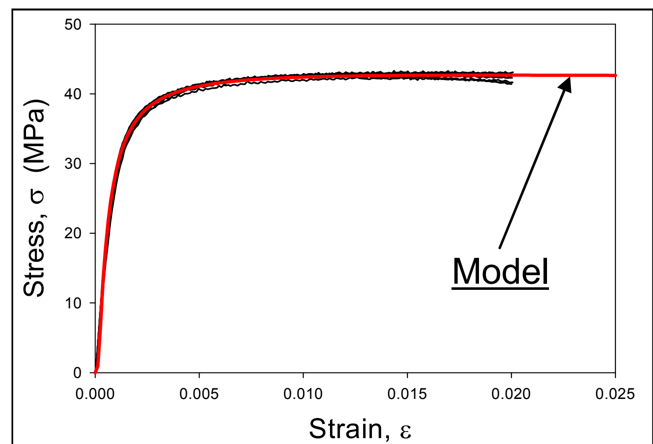

Figure 9 - Solder Stress-Strain Curves and Empirical Model

Creep Data Processing

In the solder creep experiments in our testing program, constant stress levels on the order of 25-50% of the observed UTS are being applied. For the data presented in this paper, the maximum applied stress was σ = 15 MPa, which is approximately 50% of the non-aged UTS value for the SAC305 alloy tested. Due to the long test times involved, only 5 specimens were tested for this alloy for each temperature and applied stress level. The curves for each set

of testing conditions were fit with an empirical strain-time model to generate an "average" representation of the creep response for those conditions. For the range of test conditions considered in this work, the raw strain versus time data in the primary and secondary creep regions were found to be well fit by creep response of the four parameter Burger's (spring-dashpot) model:

$$\varepsilon = \varepsilon(t) = k_0 + k_1 t + k_2 \left(1 - e^{-k_3 t}\right) \tag{4}$$

From the recorded strain vs time curves under constant stress, the "steady state" creep strain rates (k_1) have been extracted. In practice, the measured creep rate for each curve was evaluated numerically by calculating the minimum slope value in the secondary creep region of the observed $\dot{\varepsilon}$ versus t response.

ANAND VISCOPLASTIC CONSTITUTIVE MODEL

Primary Equations of Anand Model (1D)

The Anand model uses a scalar internal variable s to represent the isotropic resistance to plastic flow offered by the internal state of the material. It unifies the creep and rate-independent plastic behavior of the solder by making use of a stress equation, a flow equation, and an evolution equation. The model needs no explicit yield condition and no loading/unloading criterion.

For the one-dimensional case (uniaxial loading), the stress equation is given by

$$\sigma = c s ; \; c < 1 \tag{5}$$

where s is the internal valuable and c is a function of strain rate and temperature expressed as

$$c = c(\dot{\varepsilon}_p, T) = \frac{1}{\xi} \sinh^{-1} \left\{ \left[\frac{\dot{\varepsilon}_p}{A} e^{\left(\frac{Q}{RT}\right)} \right]^m \right\} \tag{6}$$

where $\dot{\varepsilon}_p$ is the inelastic (plastic) strain rate, T is the absolute temperature, ξ is the multiplier of stress, A is the pre-exponential factor, Q is the activation energy, R is the universal gas constant, and m is the strain rate sensitivity. Substituting eq. (6) into eq (5), the stress equation can be expressed as:

$$\sigma = \frac{s}{\xi} \sinh^{-1} \left\{ \left[\frac{\dot{\varepsilon}_p}{A} e^{\left(\frac{Q}{RT}\right)} \right]^m \right\} \tag{7}$$

Rearranging eq. (7) and solving for the strain rate yields the flow equation of the Anand model:

$$\dot{\varepsilon}_p = A e^{-\left(\frac{Q}{RT}\right)} \left[\sinh\left(\xi \frac{\sigma}{s} \right) \right]^{\frac{1}{m}} \tag{8}$$

The differential form of the evolution equation for the internal variable s is assumed to be of the form

$$\begin{aligned} \dot{s} &= h(\sigma, s, T)\dot{\varepsilon}_p \\ \dot{s} &= \left[h_o \left(1 - \frac{s}{s^*} \right)^a \text{sign}\left(1 - \frac{s}{s^*} \right) \right] \dot{\varepsilon}_p ; \quad a > 1 \end{aligned} \tag{9}$$

where the term $h(\sigma, s, T)$ is associated with the dynamic hardening and recovery processes. Parameter h_o is the hardening constant, a is the strain rate sensitivity of the hardening process, and the term s* is expressed as

$$s^* = \hat{s} \left[\frac{\dot{\varepsilon}_p}{A} e^{\left(\frac{Q}{RT}\right)} \right]^n \tag{10}$$

where $\hat{s}$ is a coefficient, and n is the strain rate sensitivity of the saturation value of the deformation resistance. For s < s*, eq. (9) can be rewritten as

$$ds = h_o \left(1 - \frac{s}{s^*} \right)^a d\varepsilon_p \tag{11}$$

and then integrated to yield

$$s = s^* - \left[\left(s^* - s_o \right)^{(1-a)} + (a-1) \left\{ (h_o) \left(s^* \right)^{-a} \right\} \varepsilon_p \right]^{\frac{1}{1-a}} \tag{12}$$

where s(0) = s_o is the initial value of s at time t = 0. Substituting eq. (10) into eq. (12) yields the final version of the evolution equation for the internal variable s:

$$s = \hat{s} \left[\frac{\dot{\varepsilon}_p}{A} e^{\left(\frac{Q}{RT}\right)} \right]^n - \left[\left(\hat{s} \left[\frac{\dot{\varepsilon}_p}{A} e^{\left(\frac{Q}{RT}\right)} \right]^n - s_o \right)^{(1-a)} + (a-1) \left\{ (h_o) \left(\hat{s} \left[\frac{\dot{\varepsilon}_p}{A} e^{\left(\frac{Q}{RT}\right)} \right]^n \right)^{-a} \right\} \varepsilon_p \right]^{\frac{1}{1-a}} \tag{13}$$

or

$$s = s(\dot{\varepsilon}_p, \varepsilon_p) \tag{14}$$

The final equations in the Anand model (1D) are the stress equation in eq. (7), the flow equation in eq. (8), and the integrated evolution equation in eq. (13). These expressions include 9 material parameters (constants): A, ξ, Q/R, m in eqs. (7, 8); and constants h_o, a, s_o, $\hat{s}$, and n in eq. (13).

Theoretical Formulation for Uniaxial Stress-Strain Response

The post yield uniaxial stress-strain relations predicted by the Anand model are obtained by substituting the expression for internal variable s from eq. (13) into the stress equation in eq. (7). The calculation results in:

$$\sigma = \frac{1}{\xi}\sinh^{-1}\left\{\left[\frac{\dot{\varepsilon}_p}{A}e^{\left(\frac{Q}{RT}\right)}\right]^m\right\}\left\{\hat{s}\left[\frac{\dot{\varepsilon}_p}{A}e^{\left(\frac{Q}{RT}\right)}\right]^n - \left[\left(\hat{s}\left[\frac{\dot{\varepsilon}_p}{A}e^{\left(\frac{Q}{RT}\right)}\right]^n - s_o\right)^{(1-a)} + (a-1)\left\{(h_o)\left(\hat{s}\left[\frac{\dot{\varepsilon}_p}{A}e^{\left(\frac{Q}{RT}\right)}\right]^n\right)^{-a}\right\}\varepsilon_p\right]^{\frac{1}{1-a}}\right\}$$

$$\sigma = \sigma(\dot{\varepsilon}_p, \varepsilon_p) \qquad (15)$$

For a uniaxial tensile test performed at fixed (constant) strain rate $\dot{\varepsilon}_p$ and constant temperature T, this expression represents highly nonlinear stress-strain behavior (power law type function) after yielding:

$$\sigma = \sigma(\varepsilon_p) \qquad (16)$$

Anand model predictions for the yield stress (σ_Y) and the Ultimate Tensile Strength (UTS = maximum/saturation stress) can be obtained by considering limiting cases of eq. (15). The UTS is given by the limit as ε_p goes to ∞:

$$UTS = \sigma\big|_{\varepsilon_p \to \infty} = \frac{\hat{s}}{\xi}\left[\frac{\dot{\varepsilon}_p}{A}e^{\left(\frac{Q}{RT}\right)}\right]^n \sinh^{-1}\left\{\left[\frac{\dot{\varepsilon}_p}{A}e^{\left(\frac{Q}{RT}\right)}\right]^m\right\} \equiv \sigma^* \qquad (17)$$

while the yield stress is given by the limit as ε_p goes to 0:

$$\sigma_Y = \sigma\big|_{\varepsilon_p \to 0} = cs_0 = \frac{1}{\xi}\sinh^{-1}\left\{\left[\frac{\dot{\varepsilon}_p}{A}e^{\left(\frac{Q}{RT}\right)}\right]^m\right\} s_0 = c\,s_0 \equiv \sigma_0 \qquad (18)$$

Using the saturation stress (σ^* = UTS) relation in eq. (17), the post yield stress-strain response (power law) in eq. (15) can be rewritten as:

$$\sigma = \sigma^* - \left[\left(\sigma^* - c\,s_0\right)^{(1-a)} + (a-1)\ \left\{\left(ch_0\right)\left(\sigma^*\right)^{-a}\right\}\varepsilon_p\right]^{1/(1-a)} \qquad (19)$$

Determination Procedure of the Model Parameters from the Stress Strain Data

As discussed above, the nine parameters of the Anand model are A, ξ, Q/R, m, h_o, a, s_o, $\hat{s}$, and n. One method to obtain the values of these parameters for a specific material is to perform a series of stress-strain tests over a wide range of temperatures and strain rates [10-11]. From the measured data, the value of the saturation stress (σ^* = UTS) can be obtained for several strain rates and temperatures. In addition, the stress-strain (σ,ε) data for each temperature and strain rate can be recast as stress vs. plastic strain data (σ,ε_p) by using

$$\varepsilon_p = \varepsilon - \frac{\sigma}{E} \qquad (20)$$

where E is the initial elastic modulus of the material at the specific temperature and strain rate being considered. The Anand model parameters can be obtained by following procedure:

1. Determine the values of the parameters $\hat{s}$, ξ, A, Q/R, n and m in by non-linear regression (least squares) fitting of eq. (17) to the saturation stress vs. strain rate and temperature data.
2. Determine the values of parameters s_o, h_o, and a by non-linear regression (least squares) fitting of eq. (19) to the stress vs. plastic strain data at several strain rates and temperatures.

Theoretical Formulation of the Anand Model for Creep Response

Substitution of the evolution expression from eq. (13) into the flow equation in eq. (8) leads to an expression relating the strain rate to the strain, applied stress, and temperature:

$$\dot{\varepsilon}_p = A e^{-\left(\frac{Q}{RT}\right)}\left[\sinh\left\{\xi\sigma\left\{\hat{s}\left[\frac{\dot{\varepsilon}_p}{A}e^{\left(\frac{Q}{RT}\right)}\right]^n - \left[\left(\hat{s}\left[\frac{\dot{\varepsilon}_p}{A}e^{\left(\frac{Q}{RT}\right)}\right]^n - s_0\right)^{(1-a)} + (a-1)\left\{(h_0)\left(\hat{s}\left[\frac{\dot{\varepsilon}_p}{A}e^{\left(\frac{Q}{RT}\right)}\right]^n\right)^{-a}\right\}\varepsilon_p\right]^{\frac{1}{1-a}}\right\}^{-1}\right\}\right]^{\frac{1}{m}} \qquad (21)$$

For a creep test at constant temperature, σ and T are constants and eq. (21) represents a highly nonlinear ordinary differential equation for the creep response. This differential equation contains all nine parameters of the Anand model and must be solved to find the creep strain vs. time relationship for a given applied stress and temperature:

$$\varepsilon_p = \varepsilon_p(t) \qquad (22)$$

Although the analytical solution of eq. (21) is not known, the equation can be solved numerically, and we have developed a Matlab code to find the numerical solution for a particular temperature and applied stress level. We have also used the coding of the Anand model into ANSYS to verify the accuracy of our Matlab numerical solutions.

The differential equation in eq. (21) for the creep response can be recast as:

$$\varepsilon_p = f\left(\dot{\varepsilon}_p\right)$$

$$\varepsilon_p = \frac{1}{c_3\left(A^{-a}\dot{\varepsilon}_p\right)^n}\left[\left\{c_2\left(A^{-1}\dot{\varepsilon}_p\right)^n - \frac{\xi\,\sigma}{\sinh^{-1}\left(c_1 A^{-1}\dot{\varepsilon}_p\right)^m}\right\}^{1-a} - \left\{c_2\left(A^{-1}\dot{\varepsilon}_p\right)^n - s_o\right\}^{1-a}\right] \qquad (23)$$

where

$$c_1 = e^{\left(\frac{Q}{RT}\right)}$$

$$c_2 = \hat{s}\left\{e^{\left(\frac{Q}{RT}\right)}\right\}^n \qquad (24)$$

$$c_3 = (a-1)\,h_0\,(c_2)^{-a}$$

Procedure for Determining the Anand Model Parameters from Creep Test Data

The nine parameters in the Anand model parameters can be determined solely from creep test data at different temperatures and stress levels by using equation (23). The solution procedure steps include:

1. Measure creep strain vs. time data for various applied stress levels and temperatures.
2. Fit the ε vs. t data for each set of testing conditions with an empirical model (e.g. Burger's model in eq. (4)).
3. Differentiate the empirical model (ε vs. t) to obtain an expression for the transient strain rate ($\dot{\varepsilon}$ vs. t) at each applied stress level and temperature
4. Express the strain as a function of strain rate, stress level, and temperature.
5. Determine the values of the model parameters by performing a nonlinear least squares regression fit of eq. (23) to the strain vs. strain rate and stress level data.

TENSILE TESTING RESULTS FOR SAC305 SOLDER

Stress-Strain Data for Various Temperature and Strain Rates

Tensile testing of SAC305 (Sn-3.0Ag-0.5Cu) lead free solder has been performed at 5 different temperatures (T = 25, 50, 75, 100, and 125 °C) and 3 different strain rates ($\dot{\varepsilon}$= .001, .0001, and .00001(1/sec)). For each set of test conditions, 10 samples were tested immediately after reflow solidification and cooldown (no aging), and eq. (2) was used to represent the measured data with an average stress-strain curve. The experimental stress-strain curves over this wide range of temperatures and strain rates were then used to extract the optimal values of the nine Anand constants for the SAC305 material.

Figure 10 illustrates measured stress-strain data for SAC305 at the 5 temperatures and 3 strain rates. Each curve in these plots represents the fit of eq. (3) to the 10 recorded raw stress-strain curves for a given set of test conditions.

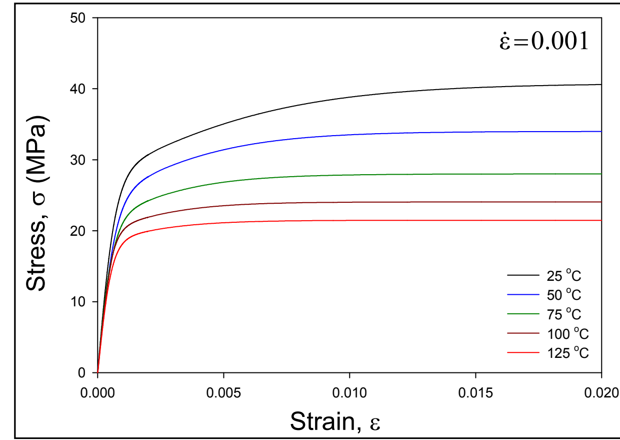

(a) $\dot{\varepsilon}$ = 0.001

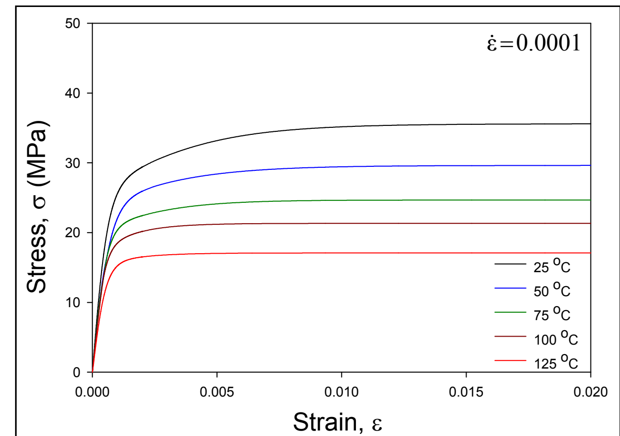

(b) $\dot{\varepsilon}$ = 0.0001

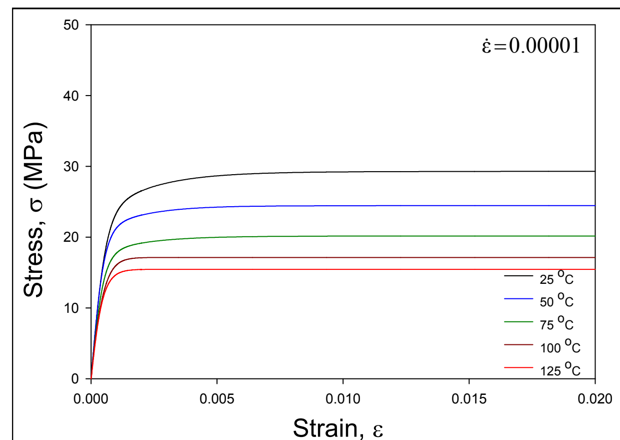

(c) $\dot{\varepsilon}$ = 0.00001

Figure 10 - Experimental Stress-Strain Curves for SAC305 [Reflowed Cooling Profile, No Aging]

The mechanical properties for the SAC305 solder have been extracted from the curves in Figure 10. Figure 11 illustrates the variation of initial effective Elastic Modulus (E), Yield Stress (YS), and Ultimate Tensile Strength (UTS) with temperature and strain rate. As expected, it is observed that all three of these properties decrease as the testing temperature increases and as the strain rate decreases. The variations were observed to be linear with temperature at all three strain rates.

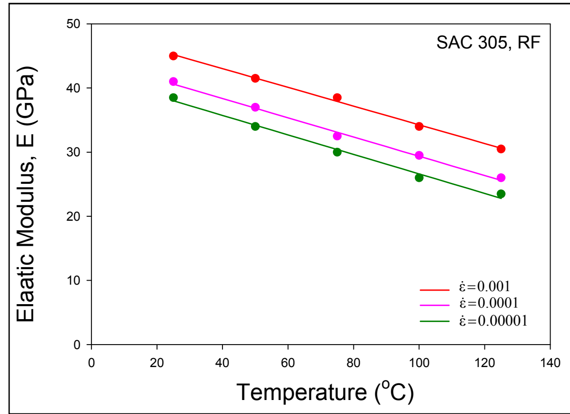

(a) Elastic Modulus

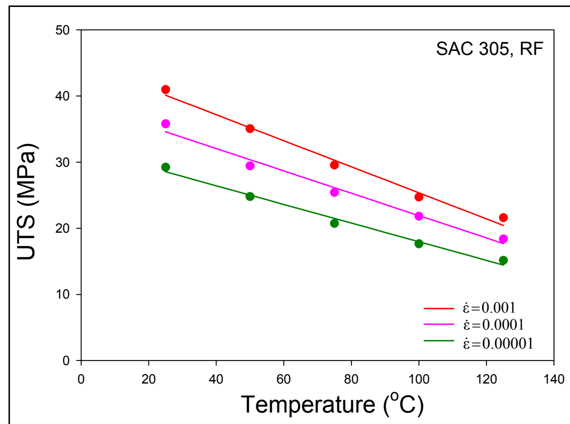

(b) UTS

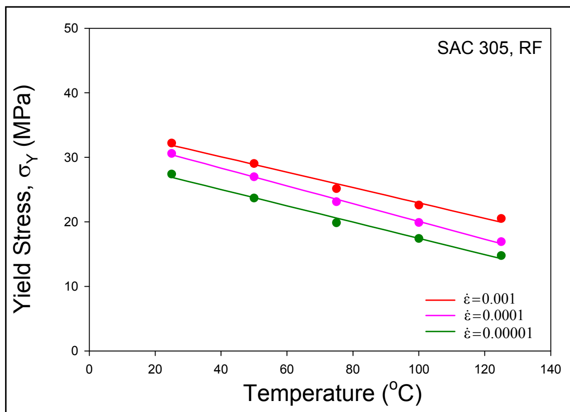

(c) Yield Stress

Figure 11 - Variation of SAC305 Material Properties with Temperature and Strain Rate [Reflowed Cooling Profile, No Aging]

Determination of Anand Model Constants from the Stress-Strain Data

Using the 2-step procedure discussed above, the nine Anand model parameters for SAC305 lead free solder have been determined from the UTS (saturation stress) data in Figure 11c, and the stress vs. plastic strain data extracted from the stress-strain curves in Figure 10. These procedures required least-squares nonlinear regression fitting, and in all cases the value of the correlation coefficient (r^2) was 0.8 or higher. The extracted Anand parameters are listed in Figure 12.

Constant Number	Anand Constant	Units	SAC305 (Stress-Strain)	SAC305 (Creep)
1	s_0	MPa	21.00	18.07
2	Q/R	1/K	9320	9096
3	A	sec^{-1}	3501	3484
4	ξ	Dimensionless	4.0	4.0
5	m	Dimensionless	0.25	0.20
6	h_o	MPa	180,000	144,000
7	$\hat{s}$	MPa	30.2	26.4
8	n	Dimensionless	0.01	0.01
9	a	Dimensionless	1.78	1.90

Figure 12 - Table of Anand Model Parameters Determined for SAC305 from Stress-Strain and Creep Data

Correlation of the Anand Model Predictions and Experimental Results for the Stress-Strain Data

Once the Anand constants were determined, it is possible to use the constitutive model to predict the stress-strain curve at each particular temperature and strain rate used in the experimental testing. The Anand model stress-strain curves could then be correlated with the experimental stress-strain curves to evaluate the goodness of fit of the constitutive model to the test data. For each temperature and strain rate, the Anand model stress vs. plastic strain response

$$\sigma = \sigma(\varepsilon_p) \tag{25}$$

was obtained from eq. (15) and the constants in Figure 12, and the stress vs. total strain response was then calculated using.

$$\varepsilon = \varepsilon_e + \varepsilon_p \qquad \varepsilon_e = \frac{\sigma}{E} \tag{26}$$

where ε is the total strain, ε_e is the elastic strain, and E is the initial elastic modulus. Figure 13 illustrates the correlation between the Anand model predictions for the stress-strain curves and the experimental data for the 5 temperatures and 3 strain rates considered. In all cases, good correlation is obtained indicating that the extracted Anand model parameter provide a good fit to the experimentally characterized response.

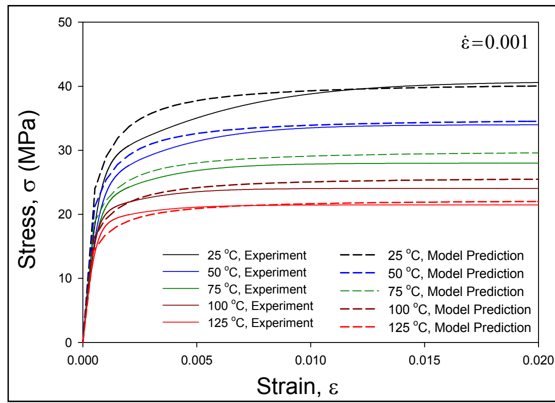

(a) $\dot{\varepsilon}$ = 0.001

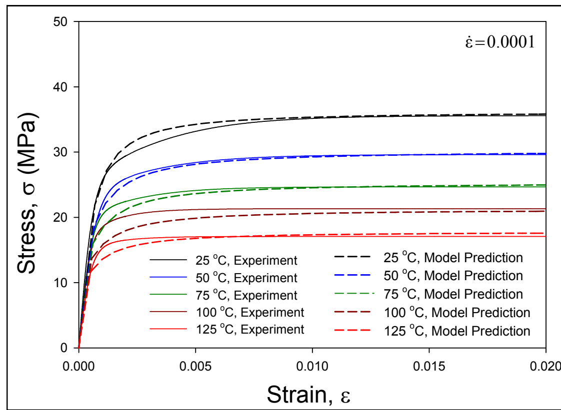

(b) $\dot{\varepsilon}$ = 0.0001

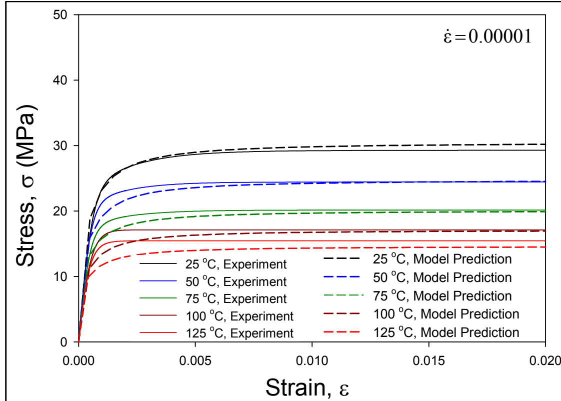

(c) $\dot{\varepsilon}$ = 0.00001

Figure 13 - Correlation of the Anand Model Predictions with Experimental Stress-Strain Curves for SAC305

CREEP TESTING RESULTS FOR SAC305 SOLDER

Creep Data for Various Stress Levels and Temperatures

Creep testing of SAC305 (Sn-3.0Ag-0.5Cu) lead free solder has been performed at 5 different temperatures (T = 25, 50, 75, 100, and 125 °C) and 3 different stress levels of (σ = 10, 12 and 15 MPa). For each set of test conditions, 6 samples were tested immediately after reflow solidification and cooldown (no aging), and eq. (4) was used to represent the measured strain vs. time data. The experimental creep curves over this wide range of temperatures and stress levels were then used to extract the optimal values of the nine Anand constants for the SAC305 material.

Figure 14 illustrates measured creep data for SAC305 at the 5 temperatures and 3 stress levels. Each curve in these plots represents the fit of eq. (4) to the 6 recorded raw creep curves for a given set of test conditions. Each graph in Figure 14 is for a particular stress level, and the various creep curves in a particular plot are for different testing temperature, illustrating the variation of the creep response with temperature.

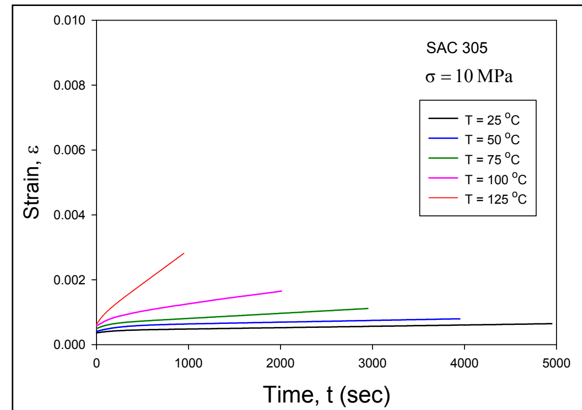

(a) σ = 10 MPa

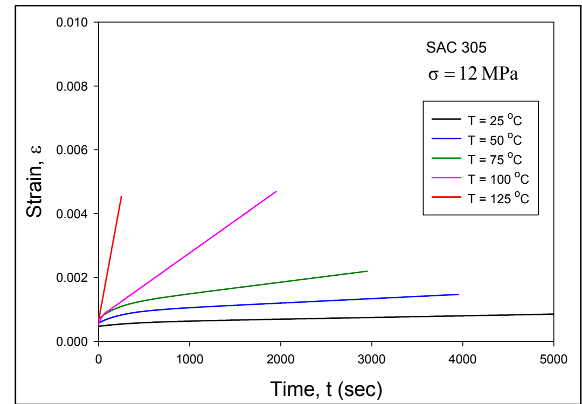

(b) σ = 12 MPa

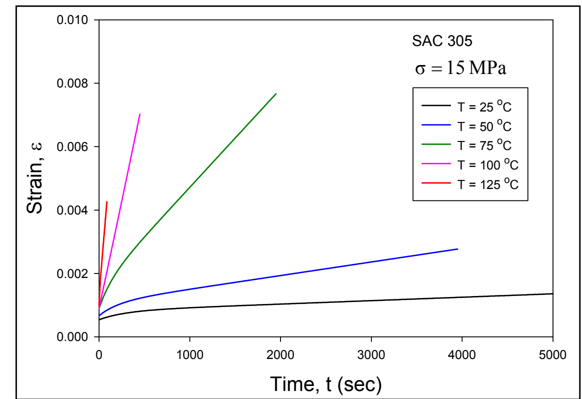

(c) σ = 15 MPa

Figure 14 - Creep Curves for SAC305 [Reflowed Cooling Profile, No Aging]

Determination of Anand Constants from the Creep Data

Using the procedure discussed above, the nine Anand model parameters for SAC305 lead free solder have been determined from the creep data in Figure 14. In order to apply the developed method to determine the Anand constants from creep data, plots of strain vs. strain rate were generated for each testing temperature and stress level. For example, Figure 15 shows ε vs. $\dot{\varepsilon}$ curves for SAC305 solder subjected to a stress level of 10 MPa and temperatures of T = 25, 50, 75, 100, and 125 °C. A non-linear least square regression method has been used to extract the Anand constants from the experimental data. The value of the correlation coefficient (r^2) in the fitting result has been obtained as 0.8 or higher. The extracted Anand parameters are listed in Figure 12.

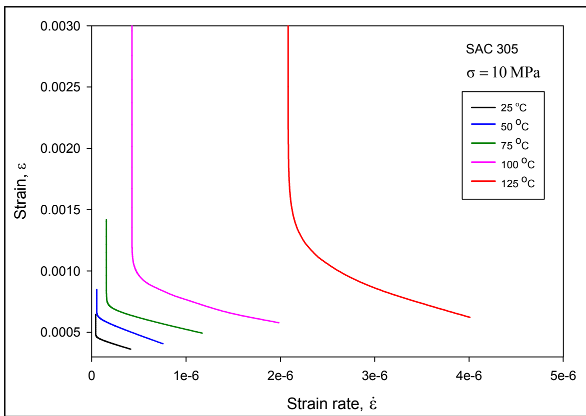

Figure 15 - Example Strain vs. Strain Rate Plots for SAC305 Solder (σ = 10 MPa)

Correlation of the Prediction of Creep Response with the Experimental Results

Once the Anand constants were determined, it is possible to use the constitutive model to predict the creep curve at a particular temperature and stress level by solving eq. (21) numerically. The Anand model creep curves could then be correlated with the experimental creep curves to evaluate the goodness of fit of the constitutive model to the test data. Figure 16 illustrates the correlation between the Anand model predictions for the creep curves and the experimental data for the 5 temperatures and 3 stress levels considered. In all cases, good correlation is obtained indicating that the extracted Anand model parameters provide a good fit to the experimentally characterized response. Also, it has been found that the nine Anand model constants determined from two methods (stress-strain and creep testing) are very close in numerical value (see Figure 12).

SUMMARY AND CONCLUSIONS

In this study, the theoretical equations for the uniaxial stress-strain response (constant strain rate) and for the creep response of solder have been derived from the Anand viscoplastic model. Procedures for extracting the Anand model constants from experimental stress-strain and creep data were also established. The two developed methods were then applied to find the Anand constants for SAC305 (Sn-3.0Ag-0.5Cu) lead free solder using two completely different sets of experimental test data. The first set of Anand parameters were extracted from uniaxial stress strain data measured over a wide range of strain rates ($\dot{\varepsilon}$ = 0.001, 0.0001, and 0.00001 1/sec) and temperatures (T = 25, 50, 75, 100, and 125 °C). The second set of Anand parameters were calculated from creep test data measured at several stress levels (σ = 10, 12 and 15 MPa and temperatures (T = 25, 50, 75, 100, and 125 °C).

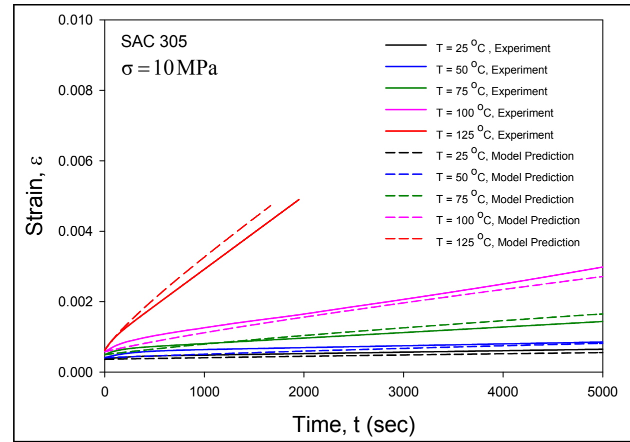

(a) σ = 10 MPa

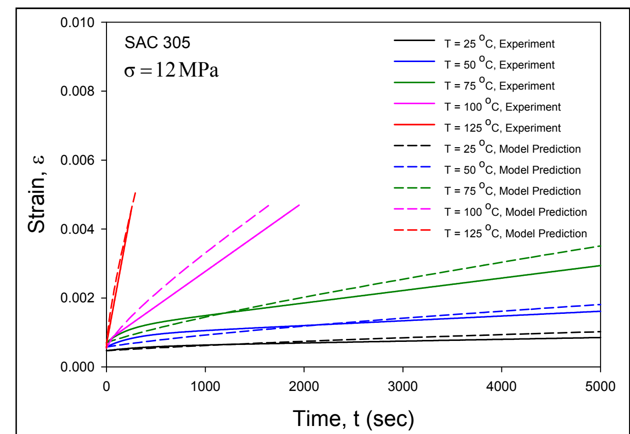

(b) σ = 12 MPa

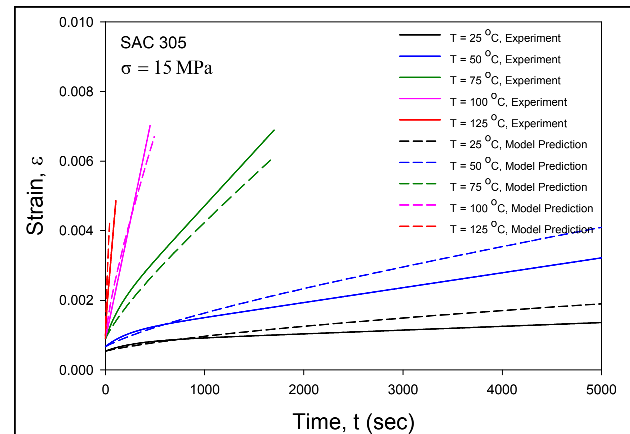

(c) σ = 15 MPa

Figure 16 - Correlation of the Anand Model Predictions with Experimental Creep Curves for SAC305

The two sets of Anand model constants derived from the stress-strain and creep data have been compared and found to be numerically very similar in magnitude. In addition, the accuracy (goodness of fit) of the Anand model using the extracted material constants has been evaluated by comparing the responses calculated from the Anand model with the measured stress-strain and creep data. In all cases, the Anand model was shown to represent the observed data very well over a wide range of temperatures and stress/strain levels.

ACKNOWLEDGMENTS
This work was supported by the US Army and the NSF Center for Advanced Vehicle and Extreme Environment Electronics (CAVE^3).

REFERENCES

1. Ma, H., and Suhling, J. C., "A Review of Mechanical Properties of Lead-Free Solders for Electronic Packaging," *Journal of Materials Science*, Vol. 44, pp. 1141-1158, 2009.
2. Solomon, H. D., "Creep Strain Rate Sensitivity and Low Cyclic Fatigue of 60/40 Solder," *Brazing and Soldering*, Vol. 11, pp. 68-75. 1986.
3. Busso, E. P., Kitano, M., and Kumazawa, T., "A Visco-plastic Constitutive Model for 60/40 Tin-lead Solder used in IC Package Joints," *Journal of Engineering Materials Technology*, Vol. 114, pp. 333-337, 1992.
4. Sung, Y., Luo, G., Kerm, S. C., "A Viscoplastic Constitutive Model for 63Sn37Pb Eutectic Solders," *Journal of Electronic Packaging,* Vol. 124, pp. 91-96, 2002.
5. Qian, Z., and Liu, S., "A Unified Viscoplastic Constitutive Model for Tin–Lead Solder Joints", *Proceedings of InterPACK '97,* ASME EEP, Vol. 19-2, pp. 1599–1604, 1997.
6. Skipor A. F., "On the Constitutive Response of 63/37 Sn/Pb Eutectic Solder", *Journal of Engineering Materials Technology*, Vol. 118(1), pp. 1–11, 1996.
7. Chen, G., and Chen, X., "Constitutive and Damage Model for 63Sn37Pb Solder under Uniaxial and Torsional Cyclic Loading", *International Journal of Solids and Structures,* Vol. 43, pp. 3596-3612, 2006.
8. R. Darveaux, K. Banerji, "Constitutive Relations for Tin-Based Solder Joints," *IEEE Transactions on Components, Hybrids, and Manufacturing Technology*, Vol. 15(6), pp. 1013-1023, 1992.
9. Pang, H. L. J., Wang, Y. P., Shi, X. Q., and Wang, Z. P., "Sensitivity Study of Temperature and Strain Rate Dependent Properties on Solder Joint Fatigue Life," *Proceedings of the 1998 Electronics Packaging Technology Conference (EPTC)*, pp.184-189, 1998.
10. Anand, L., "Constitutive Equations for the Rate-Dependent Deformation of Metals at Elevated Temperatures," *Journal of Engineering Materials and Technology*, Vol. 104(1), pp. 12–17, 1982.
11. Brown, S., Kim, K., and Anand, L., "An Internal Variable Constitutive Model for Hot Working of Metals," *International Journal of Plasticity*, Vol. 5(2), pp. 95–130, 1989.
12. Che, F., Pang, H., Zhu, W., Sun, W., and Sun, A., "Modeling Constitutive Model Effect on Reliability of Lead-Free Solder Joints", *Proceedings of the 7th International Conference on Electronics Packaging Technology,* pp. 1-6, 2006.
13. Pei, M., and Qu, J., "Constitutive Modeling of Lead-Free Solders," *Proceedings of the International Symposium on Advanced Packaging Materials,* pp. 45-49, 2005.
14. Mysore, K., Subbarayan, G., Gupta, V., and Zhang, R., "Constitutive and Aging Behavior of Sn3.0Ag0.5Cu Solder Alloy", *IEEE Transactions, Electronics Packaging and Manufacturing*, Vol. 32(4), pp. 221-232, 2009.
15. Chen, G., Chen, X., and Sakane, M., "Modified Anand Constitutive Model for Lead-Free Solder Sn-3.5Ag," *Proceedings of ITHERM 2004*, Vol. 2, pp. 447-452, 2004.
16. Amagai, M., Watanabe, M., Omiya, M., Kishimoto, K., and Shibuya, T., "Mechanical Characterization of Sn-Ag Based Lead-Free Solders," *Microelectronics Reliability*, Vol. 42(6), pp. 951-966, 2002.
17. Kim, Y., Noguchi, H., and Amagai, M., "Vibration Fatigue Reliability of BGA-IC Package With Pb-Free Solder and Pb-Sn Solder," *Proceedings of 53rd Electronic Components and Technology Conference,* pp. 891-897, 2003.
18. Bai, N., Chen, X., and Gao, H., "Simulation of Uniaxial Tensile Properties for Lead-Free Solders with Modified Anand Model," *Materials and Design,* Vol. 30, pp. 122-128, 2009.
19. Wilde, J., Becker, K., Thoben, M., Blum, W., Jupitz, T., Wang, G., and Cheng, Z., "Rate Dependent Constitutive Relations Based on Anand Model for 92.5Pb5.0Sn2.5Ag Solder," *IEEE Transaction on Advanced Packaging*, Vol. 23(3), pp. 408–414, 2000.
20. Wang, G., Cheng, Z., Becker, K., and Wilde, J., "Applying Anand model to Represent the Viscoplastic Deformation Behavior of Solder Alloys," *Journal of. Electronic. Packaging*, Vol. 123, pp. 247–247, 2001.
21. Rodgers, B., Flood, B., Punch, J., and Waldron, F., "Determination of the Anand Viscoplasticity Model Constants for SnAgCu," in *Proceedings of InterPACK 2005*, pp. 17-22, 2005.
22. Bhate, D., Chan, D., Subbarayan, G., Chiu, T., Gupta, V., and Edwards, D., "Constitutive Behavior of Sn3.8Ag0. 7Cu and Sn1.0Ag0.5Cu Alloys at Creep and Low Strain Rate Regimes," *IEEE Transactions on Components and Packaging Technology,* Vol. 31(3), pp. 622–633, 2008.
23. Ma, H., Suhling, J. C., Zhang, Y., Lall, P., and Bozack, M. J., "The Influence of Elevated Temperature Aging on Reliability of Lead Free Solder Joints," *Proceedings of the 57th IEEE Electronic Components and Technology Conference*, pp. 653-668, Reno, NV, May 29-June 1, 2007.
24. Zhang, Y., Cai, Z., Suhling, J. C., Lall, P., and Bozack, M. J., "The Effects of Aging Temperature on SAC Solder Joint Material Behavior and Reliability," *Proceedings of the 58th IEEE Electronic Components and Technology Conference*, pp. 99-112, Orlando, FL, May 27-30, 2008.

25. Zhang, Y., Cai, Z., Suhling, J. C., Lall, P., and Bozack, M. J., “The Effects of SAC Alloy Composition on Aging Resistance and Reliability,” *Proceedings of the 59th IEEE Electronic Components and Technology Conference*, pp. 370-389, San Diego, CA, May 27-29, 2009.
26. Cai, Z., Zhang, Y., Suhling, J.C., Lall, P., Johnson, R. W., Bozack, M. J., “Reduction of Lead Free Solder Aging Effects using Doped SAC Alloys,” *Proceedings of the 60th Electronic Components and Technology Conference*, pp. 1493-1511, Las Vegas, NV, 2010.
27. Mustafa, M., Cai, Z., Suhling, J., Lall, P., "The Effects of Aging on the Cyclic Stress-Strain Behavior and Hysteresis Loop Evolution of Lead Free Solders," *Proceedings of the 61st Electronic Components and Technology Conference,* Orlando, FL, pp. 927-93, 2011.
28. Motalab, M., Cai, Z., Suhling, J. C., Zhang, J., Evans, J. L., Bozack, M. J., and Lall, P., “Improved Predictions of Lead Free Solder Joint Reliability That Include Aging Effects,” *Proceedings of 62nd Electronic Components and Technology Conference*, San Diego, CA, 2012.